Crystallite size-modulated exciton emission in SnO2 nanocrystalline films grown by sputtering

Shu Sheng Pan, Siu Fung Yu, Yun Xia Zhang, Yuan Yuan Luo, Shuan Wang et al.

Citation: J. Appl. Phys. **113**, 143104 (2013); doi: 10.1063/1.4800896
View online: http://dx.doi.org/10.1063/1.4800896
View Table of Contents: http://jap.aip.org/resource/1/JAPIAU/v113/i14
Published by the AIP Publishing LLC.

Crystallite size-modulated exciton emission in SnO_2 nanocrystalline films grown by sputtering

Shu Sheng Pan,[1,2,a)] Siu Fung Yu,[2,a)] Yun Xia Zhang,[1] Yuan Yuan Luo,[1] Shuan Wang,[1] Jun Min Xu,[1] and Guang Hai Li[1,a)]
[1]*Key Laboratory of Materials Physics, Anhui Key Laboratory of Nanomaterials and Nanostructures, Institute of Solid State Physics, Chinese Academy of Sciences, Hefei 230031, People's Republic of China*
[2]*Department of Applied Physics, The Hong Kong Polytechnic University, Hung Hom, Kowloon, Hong Kong*

(Received 17 January 2013; accepted 25 March 2013; published online 10 April 2013)

SnO_2 nanocrystalline films with different crystallite sizes were grown by direct current sputtering. All the films show radiative recombination of free exciton (FX) and surface exciton (SX) with emission peaks varied from 330 to 338 nm and from 364 to 375 nm, respectively. The emission intensities of FX and SX versus crystallite size, excitation intensity, and temperature were also investigated. It was found that the emission intensities of both FX and SX increase with the decrease of the crystallite size of the films. In addition, the crystallite size has significant influence on the emission intensity of FX than SX. A model was also established to describe the relationship between crystallite size and excitonic emission intensity. From the temperature-dependent photoluminescence spectra, the activation energies of FX and SX are deduced. © *2013 AIP Publishing LLC*. [http://dx.doi.org/10.1063/1.4800896]

I. INTRODUCTION

Recent advancement in ultraviolet (UV) optoelectronic devices can be credited to the huge demand in solid-state lighting, integrated photonics, sensors, and biological applications.[1–3] Due to the wide band gap (3.6 eV) and high exciton binding energy (130 meV), tin dioxide (SnO_2) is considered to be another promising material for the realization of UV light emitting sources.[4,5] However, SnO_2 is a direct forbidden band gap semiconductor; the dipole transition between conduction band (CB) and valence band (VB) is forbidden due to the parity selection rule.[6] However, significant reduction of bulk SnO_2 into nanoscale dimensions can modify the confinement of electron wavefunction. As a result, the corresponding wavefunction parity of the CB and VB may be changed, and some transition selection rule of bulk material can be broken. Thus, radiative band-to-band transition between CB and VB is anticipated to be allowed in the SnO_2 nanostructures.[7–9] In fact, based on the density functional theory, Deng *et al*. had found that the VB maximum and CB minimum of SnO_2 quantum wires and dots have *p*- and *s*-like envelop function symmetry to permit the radiative recombination of carriers.[10]

Excitonic emission energy is dependent on the dimensions of the nanostructured SnO_2.[7,9] It is believed that the intensity of excitonic emission can be increased with the decrease of the size of the nanostructured SnO_2.[11] On the other hand, the reduction of size can also increase the influence of surface states (i.e., oxygen vacancies, undercoordinated Sn, and local disorder in the nanostructures surface areas[12]) on the excitonic characteristics of nanostructured SnO_2. Hence, the underlying correlation between dimensions and emission intensity of radiative exciton recombination are required to be understood in order to improve the emission efficiency of SnO_2 nanostructures for optoelectronic device applications.[13]

Although extensive studies on the fabrication of SnO_2 thin-film based optoelectronic devices can be found in the literature,[11] the investigation on either exciton or band-to-band radiative recombination in SnO_2 nanocrystalline films is scarce.[14–16] In addition, the correlation between the crystallite size and exciton emission intensity in SnO_2 nanocrystalline film has yet to be studied. In this paper, we report on the photoluminescence (PL) properties of SnO_2 nanocrystalline films with different crystallite sizes. In addition, it is noted that the free exciton (FX) and surface localized exciton (SX) intensities can be modulated by the variation of crystallite size. The evolution of FX and SX with excitation intensity and temperature will also be investigated.

II. EXPERIMENTAL DETAILS

The SnO_2 nanocrystalline films were grown on Si (100) wafers by direct current (DC) magnetron reactive sputtering. Tin metal plate (purity: 5N) was adopted as sputtering target; Ar (purity: 5N) and O_2 (purity: 5N) mixed gas were used as working and reacting gas, respectively. The base pressure of the chamber was lower than 5.0×10^{-5} Pa; the total work pressure was kept at 1.8 Pa. The DC power and substrate temperature were 40–60 W and 550 °C, respectively. After deposition, all the samples are annealed at 800 °C for 2 h in vacuum to enhance the crystal-quality.

The optical absorption spectra were recorded by the spectrophotometer (Varian Cary 5 E). The thickness (varies between 290 and 310 nm) of the thin films was determined by spectroscopic ellipsometry (UVISEL Jobin-Yvon). The PL spectra were collected by Edinburgh Instruments FLS920 fluorescence spectrometer excited at wavelength of 250 nm (4.96 eV) using a 450 W xenon lamp. For low-temperature

[a)]Authors to whom correspondence should be addressed. Electronic addresses: sspan@issp.ac.cn, ghli@issp.ac.cn, and sfyu21@hotmail.com

PL measurements, the samples were placed inside an Oxford liquid nitrogen cooled cryostat. The crystallographic data were obtained by X-ray diffractometer (XRD, θ-2θ, Philips X'Pert Pro MPD, Cu Kα, $\lambda = 0.1542$ nm).

III. RESULTS AND DISCUSSIONS

The crystallite size of the films in the growth direction, $D\,(= 0.9\lambda/B\cos\theta)$, can be estimated from XRD patterns using the well-known Scherrer relationship,[17,18] where λ is the X-ray wavelength, θ is the Bragg diffraction angle, and B is the full width half maximum (FWHM) after correction for instrument broadening. Due to the large crystallite size with narrow peaks, and only few diffraction peaks are arisen from the preferred orientation in the films; we adopt Scherrer relationship other than Williamson-Hall approaches to evaluate the crystallite size.[7–9] Scherrer analysis of (101) diffraction peak gives the average crystallite size of the films. The crystallite size of SnO_2 nanocrystalline films increases from 27 to 51 nm with increasing the sputtering power. Due to the conservation of energy, the energy of sputtered particles increases with an increase of sputtering power. And high-energy condensed particles have a high surface mobility to form large crystallites. The crystallite size of SnO_2 nanocrystalline films can be modified by the DC sputtering power. The XRD patterns of SnO_2 nanocrystalline films with different crystallite sizes are shown in Fig. 1(a), in which all the diffraction peaks can be indexed to the rutile SnO_2.

The room-temperature PL spectrum of SnO_2 nanocrystalline films with different crystallite sizes are shown in Figs. 1(b)–1(d). There are two dominant peaks in the UV region, as shown in Table I. The emission peaks located at 375–364 nm are attributed to the surface localized exciton at the surface region of the SnO_2 nanocrystalline in the films, and the peaks centered at 338–330 nm are originated from the free exciton recombination in the inner region from the SnO_2 nanocrystalline.[16] In our previous publication,[16] we had identified the origin and mechanism of SX and FX in SnO_2 nanocrystalline

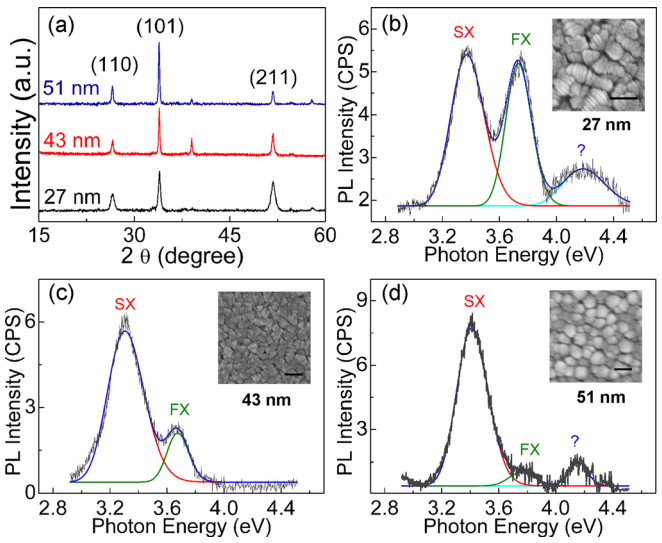

FIG. 1. PL spectra (and the corresponding SEM image) of SnO_2 nanocrystalline films with different crystallite sizes (a) 27 nm, (b) 43 nm, (c) 51 nm; (d) XRD patterns of the corresponding films.

TABLE I. PL peak energy of SnO_2 nanocrystalline films with different crystallite sizes.

Crystallite size (nm)	27	43	51
SX	367 nm (3.38 eV)	375 nm (3.31 eV)	364 nm (3.41 eV)
FX	333 nm (3.73 eV)	338 nm (3.67 eV)	330 nm (3.76 eV)
FX from QDs	297 nm (4.18 eV)	N.A.	299 nm (4.15 eV)

films. It should be pointed out that there is a weak emission band peaked at 297–299 nm in the SnO_2 nanocrystalline films with crystallite sizes of 27 and 51 nm. From the SEM image (the inset in Figs. 1(b)–1(d)), one can see that the nanocrystalline films consist of various fine grains, which are also been observed in the SnO_2 films grown by pulsed laser deposition.[19] The free excitons recombination at 270–306 nm has been observed in SnO_2 nanocrystals and quantum structures.[7,9] In a variety of nonequilibrium growth processes (e.g., sputtering process), the formation of size-distributed clusters is a very commonly encountered phenomenon.[19] In a typical DC sputtering process, the energetic Ar ions first collide with the metal target. Then, the Sn clusters ($\sim 10^3$-10^4 atoms) are generated in the sputter jet, and the SnO_2 nanocrystalline films are formed on the substrate.[20] The crystallite size has greatly influenced on the PL properties of SnO_2 nanoparticles, and the exciton emission can hardly be observed in large nanomaterials. There exists some possibility that the clusters coalesce into SnO_2 quantum dots with very fine size, which will exist in the resultant SnO_2 nanocrystalline films.[19,21] In this study, we tentatively attributed the weak luminescence at 297–299 nm to the embedded SnO_2 quantum dots inside the nanocrystalline films, and will not be discussed in this study.

From the previous investigations, one can induce that the exciton emission intensity in SnO_2 is dependent on the material dimension—"emission intensity can be increased with the reduction of size."[11] Though the theoretical calculations still lack, the enhancement of exciton emission in SnO_2 nanostructures can phenomenologically be attributed to the variation of valence and conduction band wavefunction symmetry caused by weak quantum confinement effect.

For semiconductor nanoparticles with radius R, the crystallite size $D = 2R$, the single-electron (or hole) Schrödinger equation is written as

$$-\frac{\hbar^2}{2m^*}\nabla^2\psi(r) = E\psi(r). \tag{1}$$

The eigenfunction and eigenenergy of electron (or hole) are then given as[22]

$$\psi(r) = \frac{(4\pi R^3)^{-1/2}}{j_{l+1}(\kappa_{nl})} j_l\left(\kappa_{nl}\frac{r}{R}\right) Y_l^m(\theta,\phi), \tag{2}$$

$$E = \frac{\hbar^2}{2m^*}\left(\frac{\kappa_{nl}}{R}\right)^2, \tag{3}$$

where m^* is the effective mass of electron (or hole); j_l is the l-th order spherical Bessel function; κ_{nl} being its n-th root;

$Y_l^m(\theta, \phi)$ is the spherical harmonics; and n, l, and m is the quantum numbers of the system. The boundary condition, $\psi(r) = 0$ for $r = R$, implies $J_l(\kappa_{nl}) = 0$.

From the energy-time uncertainty principle, the ΔE and Δt has a relationship: $\Delta E \Delta t \sim \hbar/2$. Based on Einstein spontaneous relationship, the transition probability p between two levels has the relationship with Δt

$$p \sim 1/\Delta t \sim \Delta E. \tag{4}$$

From the eigenenergy formula (3), the relationship between ΔE and R can be written as

$$\Delta E \propto \frac{1}{R^3} \Delta R. \tag{5}$$

The emission intensity of FX, I_{FX}, can be written as

$$I_{FX} \propto p \propto \frac{1}{R^3} \propto \frac{1}{D^3}. \tag{6}$$

Thus, the FX emission intensity is proportional to $\frac{1}{D^3}$, as shown in Fig. 2(a).

The SX comes from the recombination between conduction band tail and valence band, and the band tail states are related to the surface states in outer surface area.[16] The surface area of nanocrystals increases with the decrease of grain size, and this will induce the emission enhancement of SX originating from the surface region, as shown in Fig. 2(b). For spherical nanoparticles with average radius R, the total volume under the excitation light irradiation $N \times V_0$ is a constant value, where N is the total number of the nanocrystals and $V_0 = \frac{4}{3}\pi R^3$ is the individual nanocrystals volume. The area of all nanocrystals $N \times 4\pi R^2$ can be written as $(N \times V_0) \times \frac{3}{R}$, which is proportional to $\frac{1}{R}$. Thus, the relationship between SX emission intensity I_{SX} and crystallite size can be written as

$$I_{SX} \propto \frac{1}{R} \propto \frac{1}{D}. \tag{7}$$

The emission intensity of FX is more size-sensitive than that of SX, as shown in inset in Fig. 2(a). The typical optical absorption spectra of SnO_2 nanocrystalline film are also shown in Fig. 3(a). The typical absorption coefficient of film at 250 nm (i.e., the excitation light wavelength), α_{250}, is about $1.8 \times 10^5\,\mathrm{cm}^{-1}$. The corresponding penetration depth deduced from absorption coefficient, $1/\alpha_{250}$, is about 56 nm,

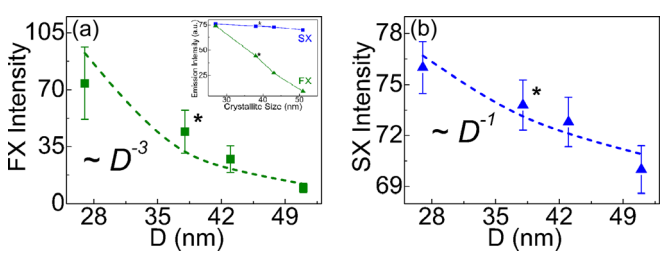

FIG. 2. Evolution and fitting curve of FX and SX with crystallite size, (a) FX and (b) SX. The inset in Fig. 2(a) shows the dependence of FX and SX emission intensities on the crystallite size; * the value taken from Ref. 16. Reprinted with permission from Appl. Phys. Lett. **97**, 221105 (2010), Copyright 2010 American Institute of Physics.

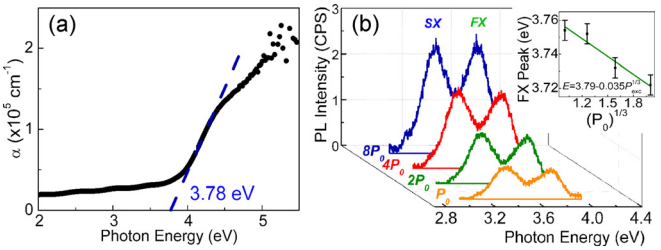

FIG. 3. (a) The typical absorption curve of SnO_2 nanocrystalline film, (b) PL spectra of SnO_2 nanocrystalline films with crystalline size of 27 nm excited at different intensities, inset: dependence of FX peak energy on $(P_0)^{1/3}$.

which is less than the film thickness (~290-310 nm). Thus, the influence of film thickness on the emission intensity of FX and SX can be neglected.

Figure 3(b) shows the PL spectra of the SnO_2 nanocrystalline film at room temperature with variation of excitation power (i.e., from P_0 to $8 \times P_0$ where $8 \times P_0$ is the strongest emission intensity of the apparatus). One can see that the peaks' intensities of both FX and SX emission increase with the increase of excitation power. The linewidth of SX and FX of the SnO_2 film with crystallite size of 27 nm becomes narrow with the increase of excitation intensity (not shown here), which has also been observed in SnO_2 nanowires and nanobelts.[23–25] The FX peak energy red shifts by 32 meV when the excitation intensity increases from P_0 to $8 \times P_0$, as shown in inset in Fig. 3(b) Due to the enhanced many body and screening effects of free carriers, the CB to VB transition peak energy will red shift with the increase of excitation intensity.[26] The first order exchange energy due to the many body effect of free electrons and holes using the Thomas-Fermi screening potential is given by

$$\Delta E_g^{exch} = \left(\frac{-2e^2 k_F}{\pi\varepsilon}\right)\left(1 + \left(\frac{\pi\kappa}{2k_F}\right) - \frac{\kappa}{k_F \tan(k_F/\kappa)}\right), \tag{8}$$

where $\kappa\,(= 2.73 \times 10^4 (\mathrm{m_e}/\mathrm{m_0})^{1/2} (n^{1/6}/\varepsilon^{1/2})\,\mathrm{cm}^{-1})$ is the reciprocal screening length, k_F $(=3.094 \times \mathrm{n}^{1/3}\,\mathrm{cm}^{-1})$ is the Fermi wave vector, $m_e(m_0)$ is the electron effective (free) electron mass, e is the electron charge, ε is the static dielectric constant, and N is the free carrier concentration.[26] Based on the fact that N is proportional to the excitation photon density, P, the relationship between carrier density and excitation density, P_{exc}, can be written as $N = yP = yP_{exc}/E_p$, where y is the quantum yield and E_p is the excitation photon energy. When $\kappa/k_F \ll 1$ due to the large N values induced by the excitation density (J/cm^3) P_{exc}, we can get an expression for PL peak energy, E

$$E = E_g(N \to 0) + \Delta E_g^{exch} = E_g(N \to 0) - \alpha P_{exc}^{1/3}, \tag{9}$$

where α is a constant. The use of Eq. (9) to fit the evolution of FX peak energy with the excitation intensity is shown in the inset in Fig. 3(b); and the corresponding fitted parameters are deduced to be $E_g(N \to 0) = 3.79\,\mathrm{eV}$ and $\alpha = 0.035\,\mathrm{eV/cm}$. The value of $E_g(N \to 0)$ value is in good agreement with the band gap E_g of the nanocrystalline thin film (i.e., 3.78 eV) as determined by optical absorption spectra measurement.

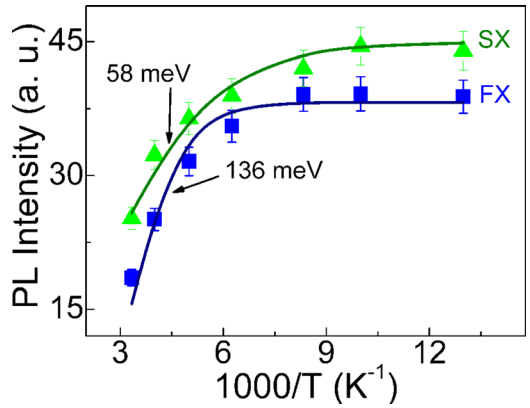

FIG. 4. Evolution of SX and FX intensities with temperature in SnO_2 films with crystalline size of 27 nm.

The temperature dependence of SX and FX emission intensities is plotted in Fig. 4. Their intensities decrease with the increase of temperature. But before 100 K, the FX and SX intensities slightly increase with increase of temperature. It is a very typical behavior for the emission from FX, which is well-known for wide band gap semiconductors.[27] The variation of FX and SX intensities with temperature can be well described by the following expression:[28]

$$I(T) = \frac{I(0)}{[1 + c\exp(-E_a/k_BT)]}, \quad (10)$$

where $c = \tau_R/\tau_0$, which is related to the radiative lifetimes of the recombination channels, τ_R is the radiative lifetime, τ_0 is a constant, E_a is the active energy for the thermal quenching process, k_B is the Boltzmann constant, and T is the temperature. The deduced activation energy of FX is 136 meV, which is well consistent with the exciton binding energy of 130 meV in bulk SnO_2. This result is evidence that the FX is from radiative recombination of free excitons. The deduced activation energy of SX is 58 meV which can be attributed to the surface donor (such as oxygen vacancy or interstitial tin) binding energy.[29] The activation energy of SX and FX is slight higher than our previous report in SnO_2 nanocrystalline film with crystallite size of 38 nm.[16] The difference may be due to the enhanced quantum confinement effect with crystallite size decreasing, which has been observed in III-V semiconductors.[30,31]

IV. CONCLUSION

Strong SX (375–364 nm) and FX (338–330 nm) emissions have been observed in SnO_2 nanocrystalline films grown by direct current sputtering. The emission intensities of FX and SX can be modulated by the crystallite size in the films, and the intensity ratio between SX and FX decreases with the decrease of crystallite size. The qualitative relationship between crystallite size and excitonic emission intensity was established. Linewidth of both FX and SX peaks reduces with the increasing of excitation intensity. The activation energy of FX and SX deduced from temperature-dependent PL intensity is 136 and 58 meV. Our results demonstrate that the controlling of the crystallite size in the SnO_2 nanocrystalline films is a facile and effective method in obtaining high-quality exciton emission.

ACKNOWLEDGMENTS

This work was financially supported by the National Natural Science Foundation of China (Grant No. 11004197), "Hong Kong Scholars Program" (Grant Nos. XJ2011039 and 201104336), PolyU Grant No. G-YZ01, and the Foundation of President of the Hefei Institute of Physical Sciences of Chinese Academy of Sciences.

[1]S. J. Jiao, Z. Z. Zhang, Y. M. Lu, D. Z. Shen, B. Yao, J. Y. Zhang, B. H. Li, D. X. Zhao, X. W. Fan, and Z. K. Tang, Appl. Phys. Lett. **88**, 031911 (2006).
[2]Y. Taniyasu, M. Kasu, and T. Makimoto, Nature **441**, 325 (2006).
[3]X. H. Huang, Z. Y. Zhan, K. P. Pramoda, C. Zhang, L. X. Zheng, and S. J. Chua, Cryst. Eng. Comm. **14**, 5163 (2012).
[4]S. Brovelli, N. Chiodini, R. Lorenzi, A. Lauria, M. Romagnoli, and A. Paleari, Nat. Commun. **3**, 690 (2012).
[5]H. Y. Yang, S. F. Yu, H. K. Liang, S. P. Lau, S. S. Pramana, C. Ferraris, C. W. Cheng, and H. J. Fan, and A. C. S. Appl. Mater. Interfaces **2**, 1191 (2010).
[6]F. J. Arlinghaus, J. Phys. Chem. Solids **35**, 931 (1974).
[7]X. Xu, J. Zhuang, and X. Wang, J. Am. Chem. Soc. **130**, 12527 (2008).
[8]S. Brovelli, N. Chiodini, F. Meinardi, A. Lauria, and A. Paleari, Appl. Phys. Lett. **89**, 153126 (2006).
[9]E. J. H. Lee, C. Ribeiro, T. R. Giraldi, E. Longo, E. R. Leite, and J. A. Varela, Appl. Phys. Lett. **84**, 1745 (2004).
[10]H.-X. Deng, S.-S. Li, and J. Li, J. Phys. Chem. C **114**, 4841 (2010).
[11]S. S. Pan and G. H. Li, Recent Pat. Nanotechnol. **5**, 138 (2011).
[12]S. O. Kucheyev, T. F. Baumann, P. A. Sterne, Y. M. Wang, T. van Buuren, A. V. Hamza, L. J. Terminello, and T. M. Willey, Phys. Rev. B **72**, 035404 (2005).
[13]L. Z. Liu, X. L. Wu, J. Q. Xu, T. H. Li, J. C. Shen, and K. C. Paul, Appl. Phys. Lett. **100**, 121903 (2012).
[14]X. J. Feng, J. Ma, F. Yang, F. Ji, F. J. Zong, C. N. Luan, and H. L. Ma, J. Cryst. Growth **310**, 3718 (2008).
[15]X. Feng, J. Ma, F. Yang, F. Ji, F. Zong, C. Luan, and H. Ma, Solid State Commun. **144**, 269 (2007).
[16]S. S. Pan, Y. H. Tian, Y. Y. Luo, Y. X. Zhang, S. Wang, and G. H. Li, Appl. Phys. Lett. **97**, 221105 (2010).
[17]X. H. Huang, Z. Y. Zhan, X. Wang, Z. Zhang, G. Z. Xing, D. L. Guo, D. P. Leusink, L. X. Zheng, and T. Wu, Appl. Phys. Lett. **97**, 203112 (2010).
[18]L. V. Azaroff, *Elements of X-Ray Crystallography* (McGraw-Hill, New York, 1968), p. 193.
[19]Z. W. Chen, J. K. L. Lai, and C. H. Shek, Appl. Phys. Lett. **88**, 033115 (2006).
[20]I. Shyjumon, M. Gopinadhan, C. A. Helm, B. M. Smirnov, and R. Hippler, Thin Solid Films **500**, 41 (2006).
[21]E. R. Leite, T. R. Giraldi, F. M. Pontes, E. Longo, A. Beltran, and J. Andres, Appl. Phys. Lett. **83**, 1566 (2003).
[22]D. Feng and G. Jin, *Introduction to Condensed Matter Physics* (World Scientific, Singapore, 2005).
[23]W. C. Zhou, R. B. Liu, Q. Wan, Q. L. Zhang, A. L. Pan, L. Guo, and B. S. Zou, J. Phys. Chem. C **113**, 1719 (2009).
[24]H. Y. Yang, S. F. Yu, S. P. Lau, S. H. Tsang, G. Z. Xing, and T. Wu, Appl. Phys. Lett. **94**, 241121 (2009).
[25]R. Liu, Y. Chen, F. Wang, L. Cao, A. Pan, G. Yang, T. Wang, and B. Zou, Physica E **39**, 223 (2007).
[26]R. A. Abram, G. J. Rees, and B. L. H. Wilson, Adv. Phys. **27**, 799 (1978).
[27]B. Liu, C. W. Cheng, R. Chen, Z. X. Shen, H. J. Fan, and H. D. Sun, J. Phys. Chem. C **114**, 3407 (2010).
[28]M. Leroux, N. Grandjean, B. Beaumont, G. Nataf, F. Semond, J. Massies, and P. Gibart, J. Appl. Phys. **86**, 3721 (1999).
[29]C. Klingshirn, *Semiconductor Optics* (Springer, Berlin, 2007).
[30]P. Ramvall, S. Tanaka, S. Nomura, P. Riblet, and Y. Aoyagi, Appl. Phys. Lett. **73**, 1104 (1998).
[31]A. D. Yoffe, Adv. Phys. **50**, 1 (2001).